Physics of Accreting Compact Binaries 2010/07/26-07/30

Observational Appearance and Spectra of Black Hole Winds

Jun Fukue and Eriko Iino (Osaka Kyoiku University

■ Abstract ■

We examine the observational appearance of an optically thick, spherically symmetric, relativistic wind (a black hole wind), focusing our attention on the emerging spectrum. In a relativistic flow, the apparent optical depth becomes small (large) in the downstream (upstream) direction due to the Lorentz-Fitzgerald contraction. As a result, the location of the apparent photosphere of the wind is remarkably modified, and there appears the relativistic limb-darkening (center-brightening) effect, where the comoving temperature distribution of the apparent photosphere is enhanced (reduced) at the center (in the limb). In addition, due to the Doppler boost, the observed temperature distribution is greatly changed. These relativistic effects modify the expected spectrum. When the wind speed is subrelativistic, the observed temperature distribution is almost uniform, and the spectra of the black hole wind are blackbody-like. When the wind speed becomes relativistic, on the other hand, the observed temperature distribution exhibits the power-law nature of $T_{obs} \propto r^{-1}$, where r is the distance from the disk center, and the observed spectra become a modified blackbody, which has a power-law part of $S_\nu \propto \nu$, where ν is the frequency.

1. Wind Model

- steady
- spherical
- velocity $v(R)=c\,\beta(R)$
- black hole mass $M=10\,M_{sun}$
- constant mass loss rate dot{m} (normalized by L_E/c^2)
- constant comoving luminosity dot{e} (normalized by L_E) = 1

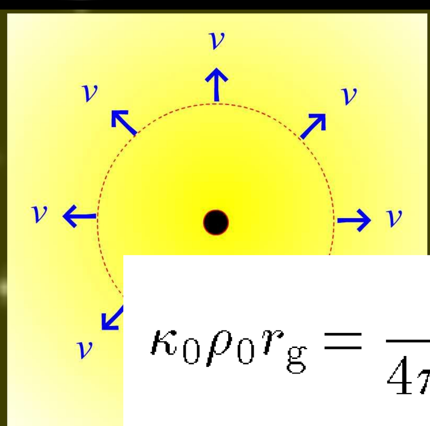

$$\kappa_0\rho_0 r_g = \frac{\dot{m}}{4\pi\gamma\beta(R)}\frac{1}{\hat{R}^2}$$

$$\frac{4\pi r_g^2\sigma T_0^4}{L_E} = \frac{\dot{e}}{\hat{R}^2}$$

2. Relativistic Optical Depth

Due to the Lorentz=Fitzgerald contraction, the relativistic optical depth in the fixed frame is modified. And we define an "apparent photosphere" of the optically thick wind as the surface, where the optical depth measured from an observer at infinity becomes unity. The observed temperature is also changed.

$$\tau_{ph} = \int_{z_{ph}}^{\infty}\gamma(1-\beta\cos\theta)\kappa_0\rho_0\,ds = 1 \qquad T_{obs} = \frac{1}{1+z}T_0 = \frac{1}{\gamma(1-\beta\cos\theta)}T_0$$

3.1 Constant－Speed Wind

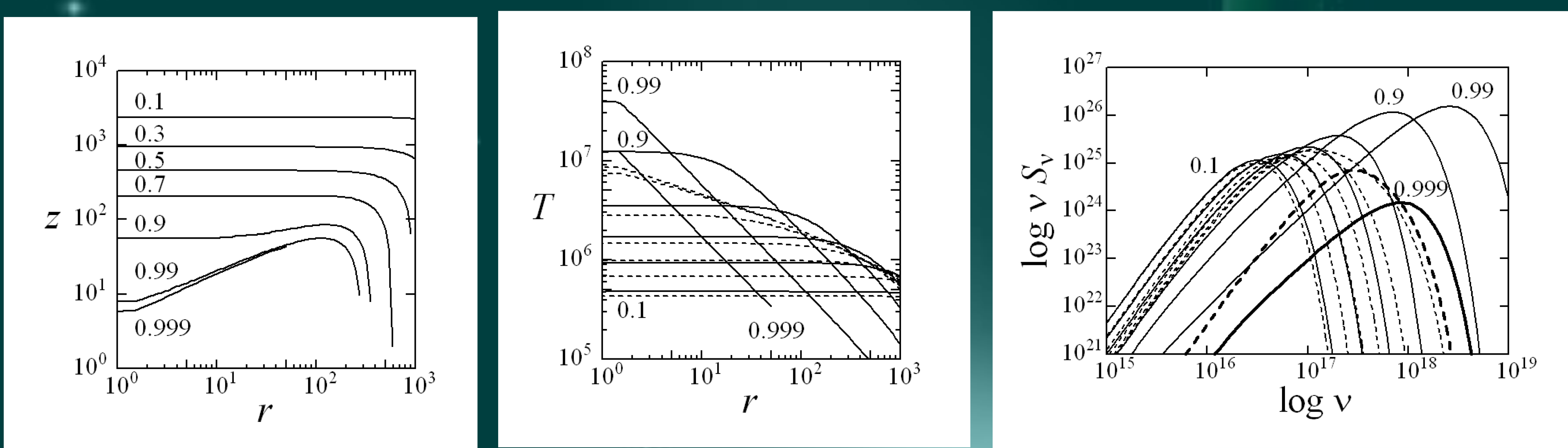

LEFT: Shape of the apparent photosphere. In the highly relativistic case the apparent photosphere becomes a concave shape for an observer in any direction.
MIDDLE: Temperature distribution at the apparent photosphere as a function of radius r. The dashed curves are the comoving temperatures, while the solid ones are the observed temperatures.
RIGHT: Expected spectra of black hole winds. The dashed curves are the comoving spectra, while the solid ones are the observed ones.
dot{m} = 1000. v/c = 0.1, 0.3, 0.5, 0.7, 0.9, 0.99, and 0.999.

Observed appearances in low and high speed cases.

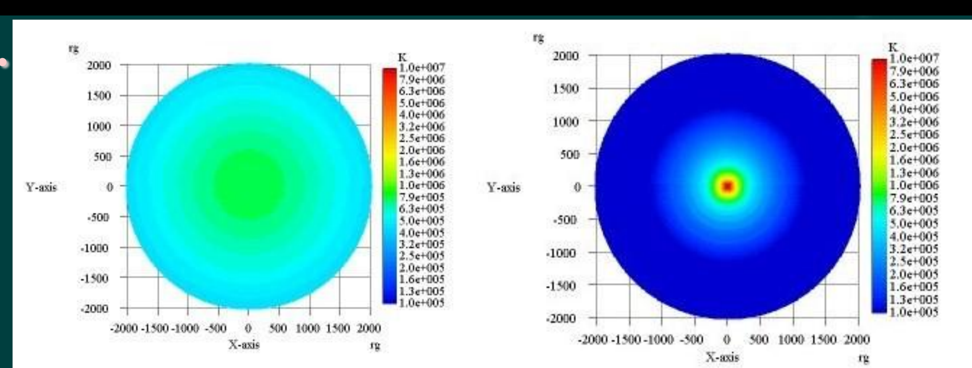

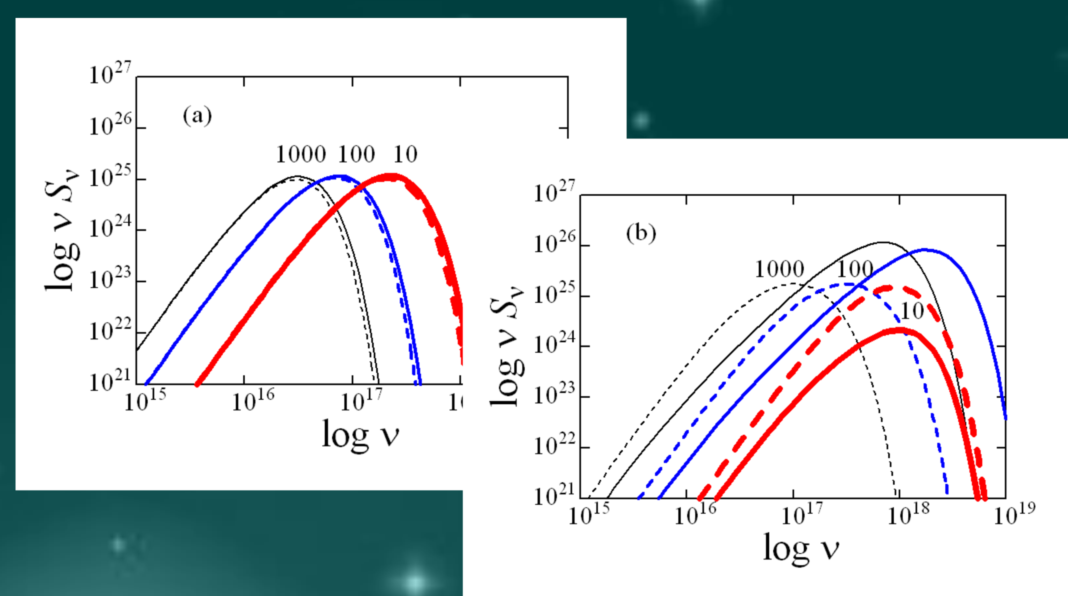

Expected spectra of for several cases.
dot{m} = 1000 (thin curves), 100 (thick curves), and 10 (very thick curves). v/c = (a) 0.1 and (b) 0.9.

3.2 Accelerating Wind

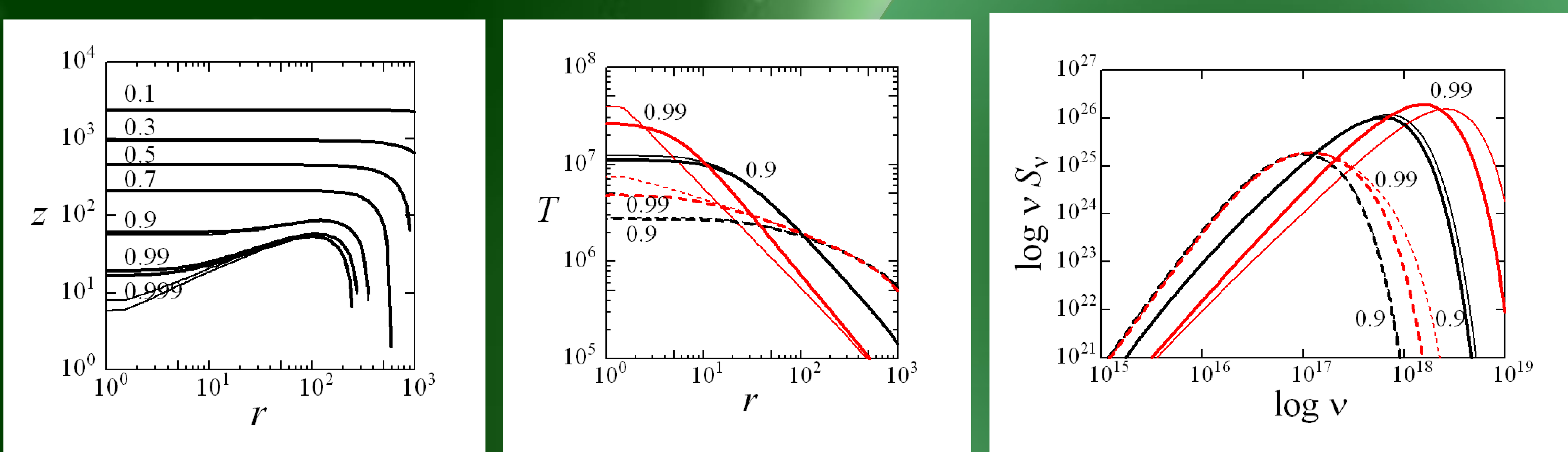

LEFT: Shape of the apparent photosphere for the accelerating (thick curves) and constant cases (thin curves).
MIDDLE: Temperature distribution of the accelerating (thick curves) and constant cases (thin curves).
RIGHT: Expected spectra of black hole winds for the accelerating (thick curves) and constant cases (thin curves).
dot{m} = 1000. v_terminal/c = 0.1, 0.3, 0.5, 0.7, 0.9, 0.99, and 0.999.

In the highly relativistic limit of $\beta \to 1$, the effective emitting region concentrates in the very center of $r \sim 0$, while z_{ph} is finite. In this case we expand (10) under the condition of $z_{ph}/r \gg 1$, and we obtain the approximate relations as

$$\hat{z}_{ph} \sim \left(\frac{\dot{m}}{4}\frac{1}{\hat{r}}\right)^{1/3}, \tag{11}$$

$$\hat{R}_{ph} = \sqrt{\hat{r}^2 + \hat{z}_{ph}^2} \sim \hat{z}_{ph}, \tag{12}$$

where the hat means that the length is normalized by the Schwarzshild radius.

Using these approximate relations, the comoving temperature distribution at around the very center is approximately expressed as

$$T_0 \propto \hat{R}^{-1/2} \sim \left(\frac{4}{\dot{m}}\right)^{1/6}\hat{r}^{-1/3}. \tag{13}$$

Similary, the observed temperature distribution at around the very center of $r \sim 0$ ($\theta \sim 0$) is approximately expressed as

$$T_{obs} \sim \frac{1}{\gamma}\frac{1}{1-\frac{z_{ph}}{R}}T_0 \sim \frac{1}{\gamma}\frac{2z_{ph}^2}{r^2}T_0 \propto \frac{2}{\gamma}\left(\frac{\dot{m}}{4}\right)^{1/2}\hat{r}^{-1}. \tag{14}$$

This is just the relation for the highly relativistic case found in the present study and shown in figure 2. For this temperature distribution, the observed spectrum automatically becomes as $S_\nu \propto \nu$ at its shoulder.

4. Concluding Remarks

In this paper we have assumed the gray atmosphere, where the opacity does not depend on frequency. Strictly speaking, the temperature should be evaluated not at the last scattering surface, but from the surface, where the effective optical depth equals to unity. In a high temperature plasma, the effective optical depth is often smaller than the total optical depth, and the gas becomes scattering dominant. In such a scattering dominated plasma, the emergent spectrum is not a simple blackbody but a modified blackbody. We should consider such a scattering effect.
In addition, in the present study we did not consider the general relativistic effect. Since the present black hole wind is optically thick, the general relativistic effect can be safely ignored in many cases. However, when the mass-loss rate is sufficiently small and/or the wind speed is very close to the speed of light, the apparent photosphere at the center shrinks down to the order of the Schwarzschild radius, and the general relativistic effect becomes important.